CRREL REPORT 96-2

Ice Accretion in Freezing Rain

Kathleen F. Jones

April 1996

Abstract

Ice accreted on structures from freezing rain causes both increased vertical loads and increased wind loads, due to the larger projected area of the structure. Structural failures initiated by ice loads frequently cause millions of dollars of damage to overhead power and communication lines, towers, and other ice-sensitive structures. There is little information on ice loads to use in the design of these structures, so freezing-rain models have been developed for use with weather measurements to determine the severity of accreted ice loads from historical data. This report describes a detailed heat-balance ice accretion model, including the important heat fluxes in freezing rain and allowing the accretion of runoff water in the form of icicles. It also presents a simple algorithm for calculating the ice load on components with different diameters and cross sections. Collision efficiency in freezing rain and the calculation of the wind-on-ice load are also discussed. Model results are compared with the ice load measured during a recent freezing rain storm, and to each other using 45 years of weather data from Des Moines, Iowa.

Cover: In this 1994 freezing-rain storm in the Southeast, ice accretions on power lines and trees caused over $100 million in damage. (Photo courtesy of Entergy.)

For conversion of SI units to non-SI units of measurement consult ASTM Standard E380-93a, *Standard Practice for Use of the International System of Units,* published by the American Society for Testing and Materials, 1916 Race St., Philadelphia, Pa. 19103.

CRREL Report 96-2

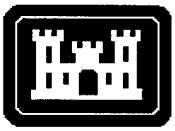

U.S. Army Corps of Engineers
Cold Regions Research & Engineering Laboratory

Ice Accretion in Freezing Rain

Kathleen F. Jones

April 1996

Prepared for
OFFICE OF THE CHIEF OF ENGINEERS

PREFACE

This report was prepared by Kathleen F. Jones, Research Physical Scientist, Snow and Ice Division, Research and Engineering Directorate, U.S. Army Cold Regions Research and Engineering Laboratory, Hanover, N.H.

Funding for this research was provided by DA Project 4A762784AT42, *Design, Construction, and Operations Technology for Cold Regions*, Work Unit CS-W03, *Alleviation of Structural Icing Effects*.

The report was technically reviewed by Dr. Edgar Andreas and Dr. Kazuhiko Itagaki of CRREL. The author wishes to thank Kim Mitchell of Entergy for providing photographs taken during the 1994 freezing rain storm in the Southeast.

CONTENTS

ILLUSTRATIONS

Figure

CONTENTS

Page

Figure (cont'd)

NOMENCLATURE

c_p specific heat of air at constant pressure = 1.006 J/g °C
c_{pc} heat capacity of the wire (J/g °C)
c_w specific heat of water = 4.22 J/g °C
C_D drag coefficient
d drop diameter (μm)
D diameter
D_c wire–ice diameter (cm)
D_i icicle diameter (cm)
dd diameter of protoicicle = 0.5 cm
$dewT$ dew-point temperature (°C)
dt time interval (s)
e_0 saturation vapor pressure of air over water at T = 0°C = 6.1121 (1.0007 + 3.46×10^{-6} Pa) mbar
e_T saturation vapor pressure of air over water at temperature T = 6.1121 (1.0007 + 3.46×10^{-6} Pa) $e^{[17.502T/(240.97 + T)]}$ mbar
f fraction of impinging precipitation that freezes to the wire
f_b fraction of runoff water that forms a protoicicle
f_s fraction of runoff water that freezes to sides of an existing icicle
g acceleration of gravity = 980 cm^2/s
Gr_L Grashof number (based on characteristic length L) = $g(0 - T)L^3/(273.15 + T)\nu_a^2$
h heat transfer coefficient (W/m^2 °C)
h_m vapor transfer coefficient (m/s)
I electric current (amp)
k_a thermal conductivity of air = 4.186×10^{-5} (573 + 1.8 T) W/m °C
L length scale for nondimensional numbers
L_{bar} average icicle length = $L_i/45$ cm
L_e latent heat of vaporization for water = 2501 J/g
L_i total icicle length (cm)
L_f latent heat of fusion for water = 334 J/g
M ice mass on wire/length (g/m)
M_i icicle mass/length of wire (g/m)
m_a molecular weight of dry air (g/mol)
m_e mass of evaporated water/length of wire (g/m)
m_w molecular weight of water vapor = 18.016 g/mol
Nu_L Nusselt number (based on characteristic length L) = hL/k_a
P precipitation rate (mm/hr)
Pa atmospheric pressure (mbar)
Pr Prandtl number = $\mu_a c_p/k_a$
P_s solar power/length (W/m)
Q_c convective heat flux (W/m^2)
Q_e evaporative heat flux (W/m^2)
Q_f latent heat flux (W/m^2)
Q_l longwave heat flux (W/m^2)
Q_k heat flux from droplet kinetic energy (W/m^2)
Q_r resistive heating flux (W/m^2)
Q_s shortwave heat flux (W/m^2)
Q_v viscous heat flux (W/m^2)
Q_w heat flux from warming impinging precipitation (W/m^2)
R gas constant = 8.31441 J/mol K
Ra_L Rayleigh number (based on characteristic length L) = $Gr_L Pr$
R_c resistance/length of conductor (ohm/m)
Re_L Reynolds number (based on characteristic length L) = LV/ν_a
R_{eq} equivalent uniform radial ice thickness (cm)
Rh relative humidity = e_{dewT}/e_T
r_v overall recovery factor for viscous heating = 0.79
S perimeter of cross section
Sc Schmidt number = ν_a/κ_m
Sh_L Sherwood number (based on characteristic length L) = $h_m L/\kappa_m$
Sr solar radiation flux (W/m^2)
T air temperature (°C)
V wind speed (m/s)
V_{load} wind load/length = $\rho_a V^2 (D_c + D_i L_i/100)/2$ N/m
$\vec{v}$ drop velocity (m/s)
W liquid water content (g/m^3)
w flux of water (g/m^2 s)

α angle from horizontal
Δt time step = 1 hour
ε ratio of the molecular weights of water vapor and air = m_w/m_a
κ_m molecular diffusivity of water vapor in air = 0.211 $[(T + 273.15)/273.15]^{1.94}$ $(1013/Pa)$ cm^2/s
μ_a dynamic viscosity of air = $1.71 \times 10^{-4} + 5.2 \times 10^{-7} T$ g/cm s
ν_a kinematic viscosity of air = μ_a/ρ_a cm^2/s
ρ_a density of air = 0.348×10^{-3} $Pa/(T + 273.15)$ g/cm^3
ρ_c wire density (g/cm^3)
ρ_i assumed density of glaze ice = 0.9 g/cm^3
ρ_o density of water = 1.0 g/cm^3
ρ_{wT} saturated vapor density at temperature T (g/cm^3)
σ Stefan–Boltzmann constant = 5.67×10^{-8} W/m^2 K^4

Ice Accretion in Freezing Rain

KATHLEEN F. JONES

1. INTRODUCTION

Freezing rain occurs throughout the United States. It may cause hazardous conditions for pedestrians and cars as the rain freezes to sidewalks and streets. The rain may also freeze to structures. Open structures that are not designed to withstand the accreted ice load and the increased wind load, due to the greater projected area of the structure, may fail. Recent severe freezing rain storms in the Midwest and the South that caused structural failures initiated by ice and wind are described in *Storm Data* (NOAA 1959–1995: Mar. 1990; Oct., Nov. 1991; Feb., Mar. 1994). Both transmission-line design guidelines (IEC 1990, ASCE 1991) and tower standards (EIA/TIA 1991) recommend designing for accreted ice, but provide little information on the ice load that should be used in design.

There have been a few nationwide and regional studies to establish the severity of freezing rain in this country. The only systematic measurements of accreted ice thicknesses in the United States are described by Bennett (1959), who presents data from nine years of measurements in the 1920s and 1930s. Tattelman and Gringorten (1973) used Bennett's data and information from *Storm Data* and its predecessors to determine ice thicknesses from freezing rain storms in the United States over a 50-year period. They then calculated extreme ice loads for return periods of up to 100 years in each of seven regions of the country. Vilcans and Burnham (1989) mapped the number of hours with freezing rain in the 24 years from 1965 to 1988 at 110 airport weather stations in the eastern half of the U.S. using archived weather data. MRI (1977) estimated ice loads on transmission lines for 25-, 50-, and 100-year return periods in Washington, Oregon, Idaho, and part of Montana using weather data with their proprietary freezing rain, snow, and rime ice accretion model. The Southeast Regional Climate Center (1993) determined the average number of freezing-rain events per year and the average event duration in Virginia, North and South Carolina, Georgia, Alabama, and Florida using archived weather information.

Hourly weather information from hundreds of weather stations across the country has been compiled at the National Climate Data Center (NCDC) and its military counterpart, the Environmental Technical Applications Center (ETAC). Weather data are available in magnetic tape format, beginning in the 1940s for some stations. These hourly measurements of the weather conditions, including precipitation rate, air temperature, dew-point temperature, wind speed, atmospheric pressure, and solar radiation, can be used with an ice accretion model to hindcast the amount of ice accreted in past freezing-rain storms.

This report describes two freezing-rain models I developed to use the historical hourly weather data. The first, described in sections 4 and 5, is a detailed heat-balance model that determines the amount of the impinging rain that freezes either directly to a structure or as icicles. The second is a simple flux model that requires only precipitation and wind-speed measurements to determine the amount of accreted ice, assuming that all the impinging water freezes. This simple model, presented in section 6, gives physical insight into the factors governing the ice load on structural elements with different cross sections. Both models are incorporated in the Microsoft FORTRAN77 program ZRAIN.* The weather parameters used in the two models are described in section 2. Ac-

*Available by request from kjones@crrel.usace.army.mil.

tual and modeled ice accretion shapes in freezing rain are discussed in section 3. The factors affecting the collision efficiency of freezing rain drops, in comparison with cloud droplets, are explained in section 7. The calculation of the wind load on an ice-covered structure using modeled ice loads is presented in section 8. Accreted ice thicknesses and masses predicted by the two models are compared in section 9.

2. HOURLY WEATHER DATA

Weather elements required in the detailed heat-balance model are

Present weather code
Wind speed
Precipitation rate
Air temperature
Dew-point temperature
Solar radiation
Atmospheric pressure.

Only present weather code, precipitation rate, and wind speed are used in the simple model. Convenient, but not consistent, units are used in ZRAIN: wind speed is in m/s, precipitation rate in mm/hr, solar radiation in W/m^2, atmospheric pressure in mbar, and air temperature and dew-point temperature in °C. The dew-point temperature, along with the air temperature, is used to determine the relative humidity of the air:

$$Rh = e_{\mathrm{dewT}}/e_{\mathrm{T}}, \qquad (1)$$

where e_{T} and e_{dewT} are the saturation vapor pressures of air over water at temperatures T and $dewT$, respectively. The diameter of the structural element on which the ice load is to be determined is specified in centimeters. Appropriate factors are incorporated in the model to convert to a consistent set of units.

Neither model predicts freezing rain. They both rely on the weather observer having indicated by the present weather code when freezing rain occurred. A number of present weather codes are used to record various intensities of freezing drizzle, freezing rain, and mixed precipitation. ZRAIN assumes that the user has screened the weather data, extracted the freezing-rain events, and summarized the occurrence of precipitation in each hour as freezing rain or drizzle (Z), mixed precipitation (+), rain (R), or snow (S) by examining the four present weather code fields in the meteorological records. The present weather code is assumed to apply for the entire hour it is reported. Only freezing rain or drizzle, rain with the air temperature below freezing, or mixed precipitation freeze to the structure. In particular, the models do not attempt to calculate the accretion of snow.

ZRAIN also requires the history of the anemometer height above ground at the weather station. The wind speed at a specified height above ground is obtained from the measured wind speed, using the anemometer height (ft) and assuming a 1/7 power law and exposure C (ASCE 1994). Typically, anemometer heights in the United States have varied between 15 and 100 ft above ground, so the correction of the wind speed to 10 m (the worldwide default anemometer height) or 30 m (typical height of a transmission-line wire) may be significant (Fig. 1). Anemometer height histories for first-order weather stations are available in *Local Climatological Data Annual Summary* (NOAA, yearly), and for military stations from ETAC in electronic format.

Solar radiation data are used to determine the solar heat flux at the accretion surface. Typically, there is little solar radiation during freezing rain because of the complete cloud cover and the relatively low solar angle in winter. During the day, solar radiation fluxes in these conditions range up to about $200\ W/m^2$, with values of about $80\ W/m^2$ more common. If solar radiation information is not available, then it can be assumed that there is no incoming solar radiation. This is true at night, but this assumption will reduce the total heat flux from the actual amount during the day and may slightly increase the hindcast ice load.

Atmospheric pressure is used in calculating the density ρ_a and saturation vapor pressure e_{T} of air and the diffusivity of water vapor in air κ_m. The dependence of these parameters on atmospheric pressure is not great. For a 50-mbar pressure change from 1000 mbar, ρ_a and κ_m change by 5% and e_{T} by only 0.02%. If atmospheric pressure data are not available, then the pressure appropriate for the elevation of the site may be assumed, with little effect on the hindcast ice load.

Most weather elements are measured every hour and are reported as an instantaneous value, rather than as an average over the hour. In the heat-balance model I assume that temperature, dew-point temperature, atmospheric pressure, and wind speed vary linearly between the reported values. In each hour there are six 10-min time

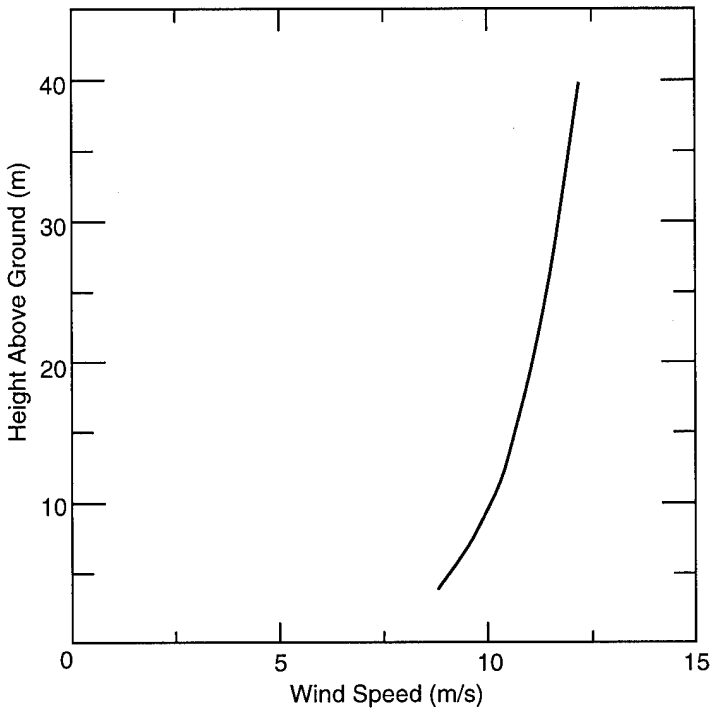

Figure 1. Wind profile for a 10-m/s wind at 10 m above ground assuming the 1/7 power law (ASCE 1994).

steps. In the first time step (e.g., 1400–1410) these weather elements take on the values reported for that hour (1400), and in the last time step (1450–1500) they are equal to the values reported for the next hour (1500). In each intermediate time step, one-fifth of the difference between the hourly values is added to the value for the previous time step. This scheme weights the reported values: each applies for 20 minutes, and the interpolated values apply for 10 minutes. Precipitation rate and solar radiation are reported as a total for the hour, and I assume them to be constant during each hour. In the simple model, the wind speed is also assumed to be constant for each hour.

A missing precipitation rate for an hour in which precipitation is reported by the present weather code is assigned 0.01 mm/hr in ZRAIN. This gives continuity to the freezing-rain event without arbitrarily adding significant mass to the accretion. If wind speed, temperature, dew-point temperature, or air pressure is missing in an hour it is assumed to be the same as in the previous hour.

The models contain no procedure for melting accreted ice. I assume, in extracting freezing-rain events from the weather data, that accreted ice melts as soon as, and only when, the air temperature rises above freezing after the freezing rain ends. The occurrence of $T > 0°C$ after freezing rain ends thus defines the end of an event. Many freezing-rain storms end with warming temperatures; however, after a well-documented ice storm in Hanover, N.H., the temperature remained cold, and accreted ice remained on wires for more than 30 days (Ackley and Itagaki 1970).

3. ICE ACCRETION SHAPE

In the models, the structure on which the ice is accreting is a horizontal circular cylinder, which is referred to as a wire in the following. Extrapolation of the models' results to other cylinder cross sections is discussed in section 6.

Ice accreted on horizontal cylinders (wires and tree branches) during freezing-rain storms in New York, Arkansas, and Vermont is shown in Figure 2 and on the cover. The shape of the ice accretions varies from a crescent on one side of a branch (Fig. 2d), to a round accretion with a few icicles (Fig. 2a), to a heavily icicled barbed-wire fence (Fig. 2b) and power line wire (cover), to an elongated accretion shape, apparently fused icicles, on a wire. The shape of accreted ice depends on the diameter of

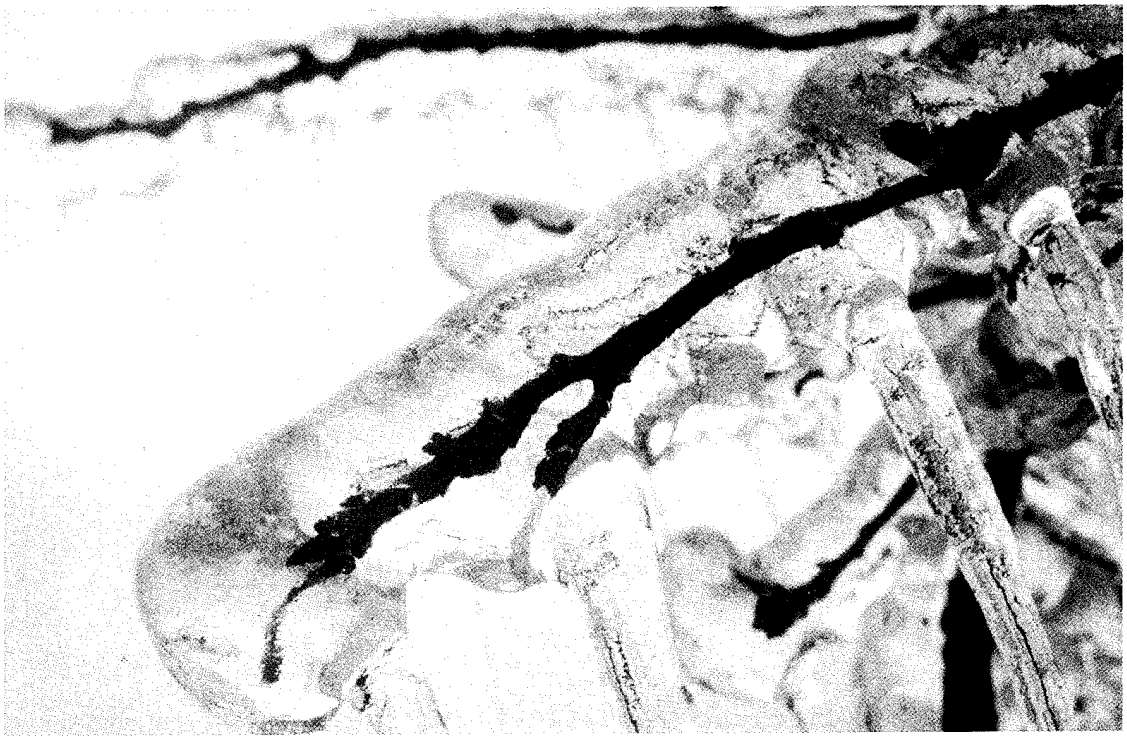

a. Tree branches, Ft. Drum, New York, March 1991 (photo, D. Fisk).

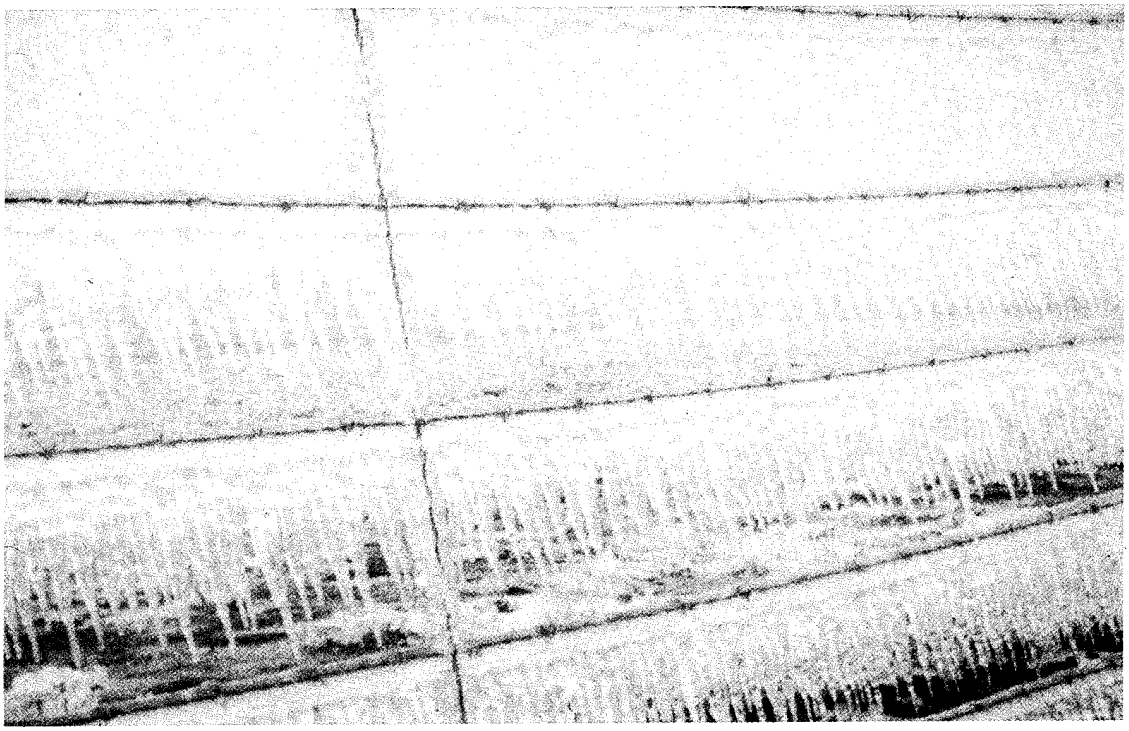

b. Barbed wire fence, Arkansas, February 1994 (photo, Entergy).

Figure 2. Freezing rain ice accretion shapes.

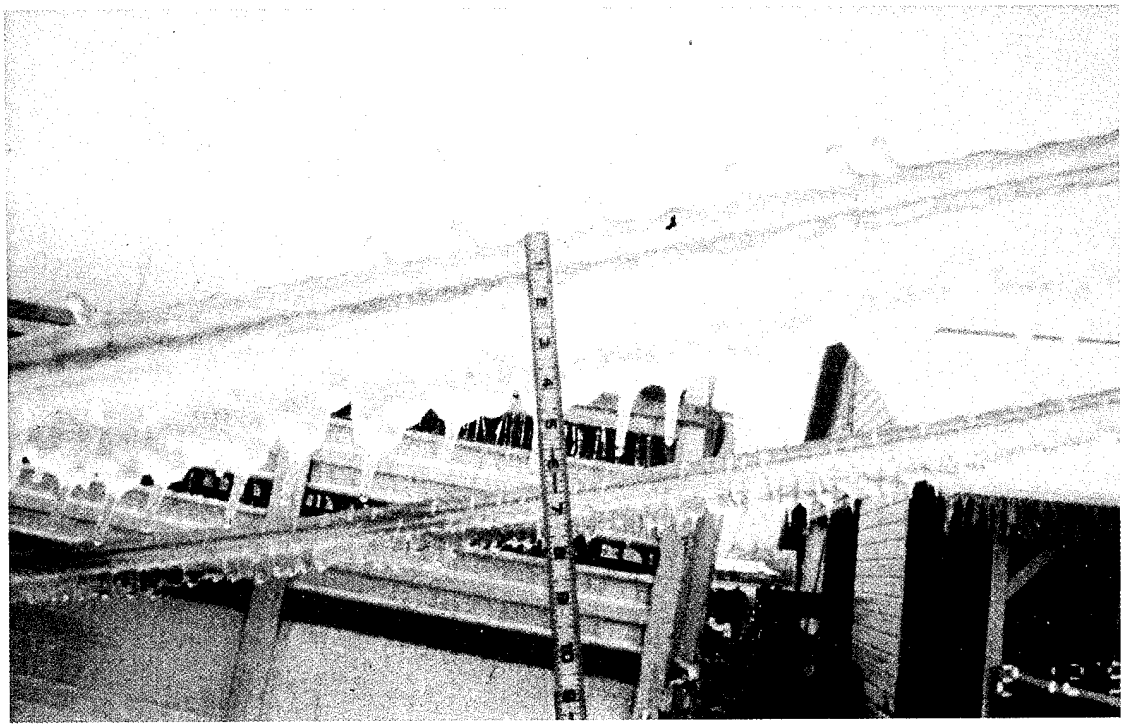

c) Wires near Dermott, Arkansas, February 1994 (photo, Entergy).

d) Tree branch, Ascutney, Vermont, February 1995 (photo, N. Mulherin).

Figure 2 (cont'd).

the wire, the rate of precipitation, the wind speed, and the rate at which the impinging water freezes. The models, however, do not attempt to determine the ice accretion shape, but instead assume simple shapes that, I hope, adequately represent reality.

In the simple flux model, the ice accretes with a uniform radial thickness around the circumference of the wire. This simple shape is consistent with the level of detail in the model.

In the heat-balance model, the precipitation that freezes immediately accretes with a uniform radial thickness. The runoff water that does not freeze immediately is allowed to freeze as icicles. The "icicle" in this model is a single, vertically oriented, circular cylinder of ice per meter of wire that can be understood as the actual icicles stacked up end to end. As runoff water freezes to the sides of the icicle, its diameter increases from an initial assumed diameter of 0.5 cm (Maeno et al. 1994). Runoff water that does not freeze to the sides of the icicle is assumed to flow down to its tip where it may freeze, in successive 0.5 cm-diameter half spheres, and increase the length of the icicle. Water that does not freeze there is assumed to drip off. At the end of each time step, the total icicle mass is distributed evenly over the new icicle length to form a uniform circular cylinder. For each 10-min time step the diameter of the wire–ice accretion D_c, and the diameter D_i and length L_i of the icicle are determined as initial conditions for the next time step.

4. HEAT BALANCE IN FREEZING RAIN

The primary process in determining the amount of the available precipitation that freezes to a structure is the flux of heat from the accretion surface. Heat must be removed from the rain drops that collide with a structure for them to freeze. In calculating the heat fluxes in the heat-balance model, the wire–ice accretion is assumed to be at 0°C. This is usually a good assumption in freezing rain because, in the typical near-freezing air temperatures, relatively low winds, and high water flux, not all the impinging precipitation freezes.

The flux of precipitation is computed using the relationship from Best (1949) to determine the liquid water content of the air as a function of the precipitation rate,

$$W = 0.067P^{0.846}, \tag{2}$$

where W is in g/m^3 and P is in mm/hr. Best reviews relationships between precipitation rate and liquid water content that both he and other researchers, including Marshall and Palmer (1948), had determined. I chose his formula rather than the Marshall–Palmer formula ($W = 0.072P^{0.88}$) for ZRAIN because it is the average of all the $W(P)$ relationships, while Marshall–Palmer's formula gives comparatively high values of W. In ZRAIN, the raindrops move horizontally at the wind speed, so the flux of precipitation w is the vector sum of the vertical and horizontal water fluxes, $P\rho_o$ and WV, respectively, converted to consistent units:

$$w(\mathrm{g/m^2s}) = \left[\left(\frac{P\rho_o}{3.6}\right)^2 + (WV)^2\right]^{1/2}. \tag{3}$$

Nine heat-flux terms were considered for inclusion in the heat-balance model to determine the fraction of the available precipitation that freezes. They are:

- Q_w (cooling flux required to warm the incoming water to 0°C) = $-c_w w(0 - T)$
- Q_c (convective cooling flux) = $-\pi h(0 - T)$
- Q_e (evaporative cooling flux) = $-10^2\pi h_m L_e[e_0/273.15 - Rhe_T/(T + 273.15)]m_w/R$
- Q_l (longwave radiative cooling flux) = $-\pi\sigma[273.15^4 - (T + 273.15)^4]$
- Q_s (shortwave radiation heat flux) = $\pi Sr/2$
- Q_f (flux of heat released by freezing all impinging precipitation) = $L_f w$
- Q_v (viscous heating flux) = $10^{-3}\pi h r_v V^2/(2c_p)$
- Q_k (heat flux from droplet kinetic energy) = $10^{-3}w\{V^2 + [P\rho_o/(3.6W)]^2\}/2$
- Q_r (resistive heating flux from current flowing through a conductor) = $10^2 I^2 R_c/D_c$.

(4)

The heat fluxes are in watts per unit length of the wire per wire–ice diameter. Q_c, Q_e, Q_l, Q_s, and Q_v all include a factor of π because they are for the outside surface of the wire–ice accretion, which has an area per unit length of π times the diameter. The magnitudes of these fluxes (except Q_r) are compared in Figure 3 for ranges of temperatures, wind speeds, precipitation rates, relative humidities, and diffuse solar radiation typical for freezing-rain events. The individual heat-flux terms are described below.

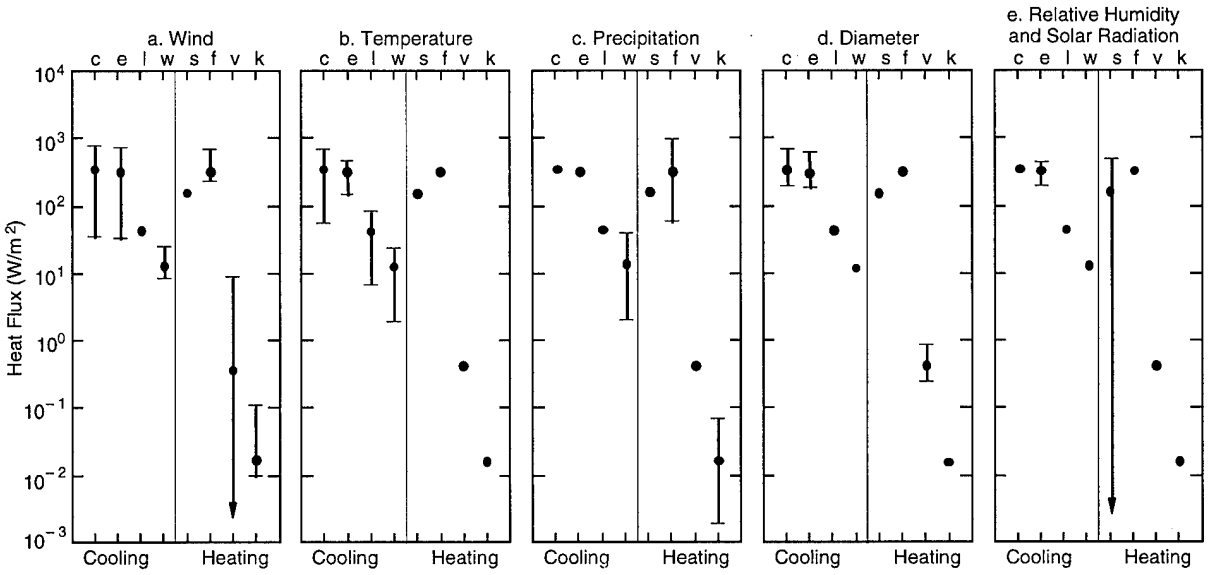

Figure 3. Comparison of heat flux terms in typical freezing-rain conditions. Standard conditions (black symbols) for the parameters are V = 3 *m/s*, T = –3 °C, P = 3 *mm/hr*, Rh = 0.90, *Sr* = 100 *W/m*^{2}, D_c = 3 *cm. In each plot one or two of these parameters is varied about the standard conditions as follows: a)* 0 < V < 10 *m/s, b)* –6 < T < –0.5 °C, *c)* 0.5 < P < 10 *mm/hr, d)* 0.5 < D_c < 10 *cm, e)* 0.80 < Rh < 1.00 *and* 0 < *Sr* < 200 *W/m*^{2}. *Minimum convective and evaporative fluxes in a) are provided by free convection. Key: e = evaporative cooling, c = convective cooling, l = longwave cooling, w = cooling from warming water, s = shortwave solar heating, f = heat of fusion, v = viscous heating, k = kinetic heating.*

Cooling flux required to warm impinging precipitation

In the heat-balance model, the latent heat of fusion given off by the fraction of precipitation that freezes to the wire warms all the impinging precipitation to 0°C. Assuming the raindrops are at the air temperature T, Q_w is the cooling flux necessary to raise their temperature to 0°C.

Convective cooling

One of the primary processes that cools the wire–ice accretion is the loss of heat from the cold air blowing past the structure. When there is no wind, heat is removed at a slower rate by free convection controlled by the temperature difference between the wire–ice accretion and the air. The Nusselt number Nu_L is used to define the rate of heat transfer in both forced and free convection in external flow:

$$Nu_L = hL/k_a, \tag{5}$$

where h is the heat transfer coefficient, L is the appropriate length scale, and k_a is the thermal conductivity of the air. In forced convection, Nu_L is given in terms of the Reynolds number Re_L and Prandtl number Pr of the flow. In free convection, where there is no external velocity scale, Nu_L is given in terms of the Rayleigh number Ra_L, which is the product of the Grashof and Prandtl numbers, Gr_L and Pr. Relationships between Nu_L and these nondimensional parameters have been determined empirically for different cylinder roughnesses and orientations.

To decide which empirical formula to use in forced convection, we need to know the typical range of Reynolds numbers for freezing rain accreting to a wire. This geometry is idealized as flow around an infinite cylinder with the wire–ice diameter (or icicle diameter) as the length scale. The smallest diameter of interest is 0.5 cm for a new icicle, and the diameter of a moderately large wire–ice accretion is about 12 cm. Typical wind speeds during freezing rain range from 0.5 to 10 m/s, and the kinematic viscosity of air is ν_a = 0.132 cm^2/s at 0°C. Using these values, the Reynolds number range of interest is $190 < Re_D < 9.1 \times 10^4$, where D is the diameter of either the icicle or the wire–ice accretion.

Achenbach (1977) determined the total Nusselt number for rough cylinders in subcritical flow, for $Re_D > 10^4$ with air (Pr = 0.72) as the fluid, as

$$Nu_D = 0.18\ Re_D^{0.63}. \quad (6)$$

In these wind-tunnel experiments, the cylinder surface was maintained at a constant temperature. The cylinders were roughened to three different roughness heights by knurling the surface into regular pyramidal shapes. The data showed that, in subcritical flow, Nu_D is independent of the roughness height, but the upper value of the Reynolds number for subcritical flow varies between 2×10^5 and 10^6, decreasing with increasing roughness. The higher Reynolds numbers for ice accretions in freezing rain are below the upper value of this subcritical flow range, but the lower values of Re_D extend well below 10^4, the lower limit in Achenbach's (1977) experiments. To obtain appropriate Nusselt numbers for these lower Reynolds number conditions, I used results from Morgan (1973). He determined Nu_D for bare, stranded conductors for $Re_D > 10^2$, maintaining a constant heat flux rather than a constant surface temperature. He compared these stranded conductor results to his Nusselt number formulation for smooth cylinders in Morgan (1975). Morgan's and Achenbach's results and a formula determined for smooth cylinders by Zhukauskas and recommended in Incropera and DeWitt (1985) are compared in Figure 4. This figure shows that Zhukauskas's smooth cylinder formula predicts Nusselt numbers that are lower than Morgan's data at low Reynolds numbers and lower than Achenbach's at high Reynolds numbers. The scatter of the wind-tunnel data in this figure illustrates the uncertainty in determining the Nusselt number for real freezing-rain ice accretions with irregular roughness that is different from that in both Achenbach's and Morgan's controlled experiments. I incorporated Morgan's and Achenbach's rough cylinder results in the heat-balance model as follows:

$$\begin{aligned} Nu_D &= 0.583\ Re_D^{0.471} && 35 < Re_D < 1600 \\ Nu_D &= 0.18\ Re_D^{0.63} && 1600 < Re_D \leq 1 \times 10^6 \\ Nu_D &= 0.00257\ Re_D^{0.98} && Re_D > 1 \times 10^6, \end{aligned} \quad (7)$$

extrapolating Achenbach's formula to lower

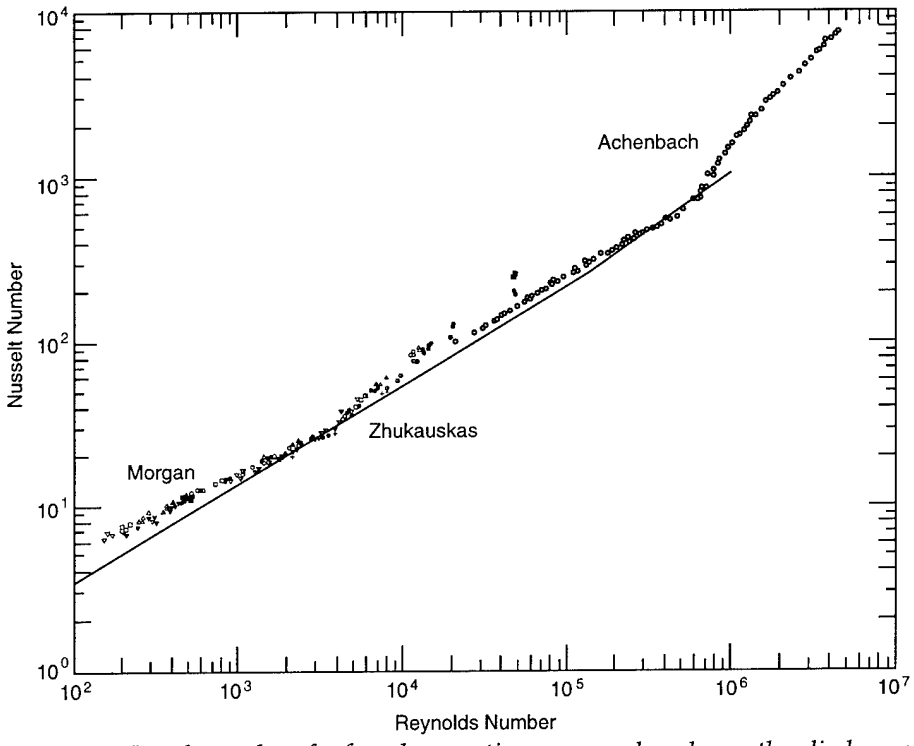

Figure 4. Nusselt numbers for forced convection over rough and smooth cylinders as a function of Reynolds number. Rough cylinder data from Achenbach (1977) are for Reynolds numbers larger than 10^4. Morgan's (1973) rough cylinder data are for Reynolds numbers less than 5×10^4. Zhukauskas's curve (Incropera and DeWitt 1985) is for smooth cylinders for the entire range of Reynolds numbers shown.

Reynolds numbers to intersect Morgan's at Re_D = 1600. In Morgan's formula for Nu_D, ν_a and ρ_a are supposed to be determined at the average of the wire–ice surface temperature (0°C) and the air temperature T. However, these temperatures typically differ by only a few degrees in freezing rain, so there is very little error in using the air temperature in calculating these parameters.

Both Achenbach's and Morgan's experiments were done in air, and neither specified the dependence of Nu_D on the Prandtl number. For air at the temperatures and pressures appropriate for freezing rain, Pr is essentially constant. Following Zhukauskas (Incropera and DeWitt 1985), I assume that Nu_D is proportional to $Pr^{0.37}$. Thus eq 7 can be written

$$\begin{aligned} Nu_D &= (0.583/Pr^{0.37})\, Pr^{0.37}\, Re_D{}^{0.471} \\ &\quad 35 < Re_D < 1600 \\ Nu_D &= (0.18/Pr^{0.37})\, Pr^{0.37}\, Re_D{}^{0.63} \\ &\quad 1600 < Re_D < 1\times 10^6 \\ Nu_D &= (0.00257/Pr^{0.37})\, Pr^{0.37}\, Re_D{}^{0.98} \\ &\quad Re_D > 1\times 10^6. \end{aligned} \tag{8}$$

This formulation is used with the heat and mass transfer analogy in determining the evaporative cooling flux.

Evaporative cooling

Under typical freezing-rain conditions, the impinging water does not freeze immediately. There is a vapor density gradient away from the wire because the wire–ice surface is warmer than the air and the saturation vapor density increases with temperature. This gradient is enhanced if the relative humidity of the air is less than 100%. Thus, the water film on the surface of the wire–ice accretion is evaporating as it freezes and cooling the remaining water. The evaporative cooling flux is

$$Q_e = -10^2 \frac{L_e m_e}{D_c dt} = -10^6 \pi L_e h_m \Delta\rho_w , \tag{9}$$

where L_e is the latent heat of evaporation, m_e is the mass of evaporated water per unit length, D_c is the wire–ice diameter, dt is the time interval, h_m is the vapor transfer coefficient, and $\Delta\rho_w$ is the vapor density difference between the ice accretion surface and the air. The vapor density ρ_{wT} is related to the saturation vapor pressure e_T by the ideal gas law

$$\frac{e_T m_w}{\rho_{wT}} = 10^4 R(T + 273.15) , \tag{10}$$

to give

$$\begin{aligned} \Delta\rho_w &= \rho_{w0} - Rh\rho_{wT} \\ &= 10^{-4}\left(\frac{e_0}{273.15} - \frac{Rhe_T}{T+273.15}\right)\frac{m_w}{R}, \end{aligned} \tag{11}$$

where m_w is the molecular weight of water vapor, R is the gas constant, Rh is the relative humidity, and e_T and e_0 are the saturation vapor pressures at temperatures T and 0°C, respectively. This formulation for Q_e is compared with that in other ice accretion models in Appendix A.

The empirical formula used in the heat-balance model for the saturation vapor pressure over water,

$$\begin{aligned} e_T = 6.1121(1.0007 &+ \\ 3.46\times 10^{-6} Pa) &e^{17.502T/(240.97+T)}, \end{aligned} \tag{12}$$

is from Buck (1981). The saturation vapor pressure over water, rather than over ice, is used, both in the air and at the accretion surface, because both the precipitation and the accretion surface are unfrozen.

The vapor transfer coefficient h_m is determined using the mass and heat transfer analogy (Incropera and DeWitt 1985). The nondimensional number for mass transfer equivalent to Nu_L for heat transfer is the Sherwood number $Sh_L = h_m L/\kappa_m$ where κ_m is the vapor diffusivity. The Schmidt number $Sc = \nu_a/\kappa_m$ is equivalent to Pr. Like Pr, Sc is virtually constant for air at the temperatures and pressures we are concerned with. The heat and mass transfer analogy states that for any function $Nu_L(Re_L, Pr)$ the Sherwood number is the same function of Re_L and Sc. Thus, for mass transfer the equivalent to eq 8 is

$$\begin{aligned} Sh_D &= (0.583/Pr^{0.37})\, Sc^{0.37}\, Re_D{}^{0.471} \\ &\quad 35 < Re_D < 1600 \\ Sh_D &= (0.18/Pr^{0.37})\, Sc^{0.37}\, Re_D{}^{0.63} \\ &\quad 1600 < Re_D < 1\times 10^6 \\ Sh_D &= (0.00257/Pr^{0.37})\, Sc^{0.37}\, Re_D{}^{0.98} \\ &\quad Re_D > 1\times 10^6. \end{aligned} \tag{13}$$

The vapor transfer coefficient $h_m = (Sh_D\kappa_m)/D$ is then obtained from eq 13 for the appropriate Reynolds number range. Significantly different values for vapor diffusivity κ_m are specified in different references. Incropera and DeWitt (1985) give κ_m = 0.26 cm^2/s at T = 25°C and Pa = 1000 mbar in their Table A8. They also say κ_m is proportional to $(T + 273.15)^{3/2}$, which results in κ_m = 0.23 cm^2/s at 0°C. Batchelor (1970, Appendix 1) specifies κ_m = 0.25 cm^2/s at 15°C. Pruppacher and Klett

(1980, p. 413) give

$$\kappa_m = 0.211\left(\frac{T+273.15}{273.15}\right)^{1.94}\left(\frac{1013}{Pa}\right)\mathrm{cm}^2/\mathrm{s}, \quad (14)$$

which results in $\kappa_m = 0.21\ \mathrm{cm}^2/\mathrm{s}$ at $Pa = 1000$ mbar and $T = 0°C$. They also say that conventionally used values may be too high, and as they are a better source for this information than either Incropera and DeWitt (1985) or Batchelor (1970), their formula for κ_m is used in the heat-balance model.

The mass of water that evaporates in the process of freezing the impinging rain is $m_e = -10^{-2}Q_eD_c dt/L_e$ (eq 9). In the heat-balance model, the evaporated water is subtracted from the runoff water available for icicle formation if not all the impinging precipitation freezes directly to the wire.

Convective and evaporative cooling in no wind

When there is no wind there cannot be forced convection, so convective heat transfer occurs by free convection only. Free convection occurs when the temperature difference between the wire–ice accretion and the air causes the air column to be unstable. The wire–ice accretion is typically warmer than the ambient air, so the warmer air over the wire rises and is replaced continuously by colder air. Heat transfer in free convection is governed by the Grashof number,

$$Gr_L = \frac{g(0-T)L^3}{(273.15+T)\nu_a^2}, \quad (15)$$

and the Rayleigh number,

$$Ra_L = Gr_L Pr = \frac{g(0-T)L^3\rho_a c_p}{(273.15+T)\nu_a k_a}, \quad (16)$$

where g is the acceleration of gravity, c_p is the specific heat of air, and ν_a is the kinematic viscosity of air. It can be assumed that forced and free convection do not occur simultaneously when Re_L/Gr_L^2 is much different from 1 (Incropera and DeWitt 1985). For typical wire–ice diameters, wind speeds, and air temperatures in freezing rain, $Gr << Re^2$, so this is a good assumption. I assume in the heat-balance model that forced convection controls the heat transfer if there is any wind, and free convection controls only when there is no wind ($V = 0$). The Nusselt number determined by Morgan (1975) for free convection around smooth horizontal cylinders is

$$\begin{aligned} Nu_{Dc} &= 0.85\ Ra_{Dc}^{0.188} \quad 100 < Ra_{Dc} < 10^4 \\ Nu_{Dc} &= 0.48\ Ra_{Dc}^{0.250} \quad 10^4 < Ra_{Dc} < 10^7. \end{aligned} \quad (17)$$

In a separate paper, Morgan (1973) argues that for relatively low Rayleigh numbers ($100 < Ra < 4\times10^5$), the roughness of the surface does not have an effect on heat transfer, so these formulas should also apply to rough ice accretions. For most reasonable combinations of the wire–ice accretion diameter and weather parameters in freezing rain, the Rayleigh number is within this low range, so eq 17 are incorporated in the heat-balance model to determine the heat transfer coefficient for the wire when there is no wind.

The heat and mass transfer analogy can be used in free convection (Incropera and DeWitt 1985) to estimate the mass transfer coefficient for evaporative cooling from eq 17:

$$\begin{aligned} Sh_{Dc} &= 0.85\ Ra_{Dc}^{0.188}\,(Sc/Pr)^{0.188} \\ &\qquad 100 < Ra_{Dc} < 10^4 \\ Sh_{Dc} &= 0.48\ Ra_{Dc}^{0.250}\,(Sc/Pr)^{0.250} \\ &\qquad 10^4 < Ra_{Dc} < 10^7. \end{aligned} \quad (18)$$

Longwave radiative cooling

In computing the flux of longwave radiation for the heat-balance model, I assume that the wire–ice accretion is radiating at 0°C and the clouds and surrounding rain-filled air are radiating at the air temperature T. The emissivity of everything is taken to be 1 [emissivity of ice is 0.98 and of water is 0.96 (Incropera and DeWitt 1985)]. Then the longwave cooling flux is given by the blackbody radiation law:

$$Q_l = -\pi\sigma[273.15^4 - (T+273.15)^4]. \quad (19)$$

Shortwave radiative heating

The shortwave heat flux $Q_s = \pi Sr/2$ is determined using the measured or modeled incoming global diffuse radiation flux Sr. This information is available hourly at some weather stations (NOAA 1993) and is reported as an average for each hour. The factor of $\pi/2$ transfers the reported values for a flat horizontal surface to a horizontal cylinder. The derivation of this factor is presented in Appendix B. I assume in the heat-balance model that the albedo of the wire–ice accretion is zero (the ice is clear), that all the incoming radiation to the accretion is absorbed in either the ice or the underlying wire, and that there is no radiation reflected back from the ground to the wire. These assumptions are only approximately correct, but they are somewhat offsetting in their simplicity: a) the al-

bedo of the ice is close to, but greater than zero, and depends on how much air and/or snow is incorporated in the accretion, b) the shorter-wavelength visible radiation may not be absorbed in the ice, but it is probably absorbed in the underlying wire, which is assumed to be in thermal equilibrium with the ice accretion, and c) the ground surface reflects some incoming radiation, depending on the ground cover and the amount and condition of snow and ice on the ground.

The shortwave and longwave fluxes are opposite in sign and comparable in size, but there is no shortwave flux at night, when the air temperature may be relatively cold and the longwave flux relatively large. Both are small compared with the convective and evaporative fluxes in typical freezing-rain conditions, but large compared with the viscous and kinetic heat fluxes (Fig. 3).

Viscous heating

The formula for the viscous heat flux is from Makkonen (1984). At wind speeds appropriate for freezing rain, viscous heating from air moving by the wire–ice accretion is small compared with the other heat fluxes (Fig. 3). This term is not included in the heat-balance model.

Kinetic heating

When precipitation drops collide with the wire–ice accretion, some of their kinetic energy is converted to heat. At the droplet speeds associated with freezing rain, this term is small (Fig. 3). It is not included in the heat-balance model.

Resistive heating

If the wire conducts electricity, heat is generated from the wire resistance. The resistive heat generated per unit length of wire I^2R_c depends on the current I and the wire resistance per meter R_c, which generally is a function of the current load and frequency. The resistive heat flux per wire diameter is

$$Q_r\,(\mathrm{W/m^2}) = \frac{10^2 I^2 R_c}{D_c} \,. \qquad (20)$$

The resistive heat flux in a wire varies from zero, when there is no current, up to values larger than any of the other heating or cooling fluxes. For example, for a 2.63-cm (1.036-in.)-diameter ACSR conductor with I = 400 amp and $R_c = 8.14 \times 10^{-5}$ ohm/m (0.131 ohms/mile), Q_r = 490 W/m^2. This is comparable to the typical convective and evaporative cooling fluxes in freezing rain shown in Figure 3. Because of the extremely large range in the resistive heating flux and because assuming no resistive heating is both reasonable and conservative, it is not included in the model.

Latent heat of fusion

To freeze water at 0°C, the heat of fusion must be removed. The fraction f of the impinging precipitation that freezes is the ratio of the sum of all the other heat fluxes to the latent heat flux Q_f that is calculated assuming that all the incoming water freezes:

$$f = \frac{Q_c + Q_e + Q_l + Q_s + Q_w}{Q_f} \,. \qquad (21)$$

If f is 1 or greater, then all the incoming water freezes. Properly, the temperature of the accretion surface should be determined iteratively, and heat-flux terms for cooling the ice to the calculated surface temperature and depositing hoarfrost or sublimating accreted ice should be included. These are small effects in freezing-rain conditions, however, and are not incorporated in the heat-balance model.

Other effects

Two other, possibly significant, factors in determining the heat balance at the ice accretion surface are a) the angle of the wire to the wind direction, and b) freezing of the impinging precipitation by the cold stored in the wire.

Wind direction is archived with the weather data, so for a particular structure the yaw of the wire to the wind direction during freezing rain could be determined. The wire orientation could then be incorporated in the calculation of the precipitation flux w across the wire by multiplying the righthand side of eq 3 by the sine of the angle between the wire and the direction of the precipitation flux. The Nusselt number also depends on the yaw of the wire. Morgan (1973, 1975) discusses the variation of the Nusselt number with yaw in forced convection for both smooth cylinders and bare, stranded wires.

If the air temperature is cold before freezing rain begins and the wire is in equilibrium with the air, impinging precipitation may freeze by conductive heat loss into the wire. The mass of water that can be frozen by this mechanism is

$$M = -\frac{10^2 \pi D_c^2 \rho_c c_{pc} T}{4 L_f} \,, \qquad (22)$$

where ρ_c is the density and c_{pc} is the heat capacity of the wire. This effect is small except perhaps for

large structural elements. For example, for a 3-cm-diameter aluminum wire, with $c_{pc} = 0.88$ J/g° C, ρ_c = 2.77 g/cm^3, and air temperature $T = -5$°C, the mass of water that can be frozen by heat conduction into the wire is 26 g/m, which is equivalent to an ice thickness of 0.03 cm. The calculation of this additional mass of ice is included as an option in the model.

5. ICICLES

Precipitation that does not freeze to the wire may freeze as icicles in the process of dripping off the wire. I assume that there is no precipitation impinging directly on the icicles. At low wind speeds, icicles form directly under the wire and are shielded by the wire from the falling rain. At high wind speeds, the runoff water is blown to the lee side of the wire so icicles form behind the wire, shielded from the wind-driven rain. In the heat-balance model, a single icicle per meter of wire represents the actual icicles on that meter of wire stacked end to end. If there is no existing icicle, the mass of water that is not frozen or evaporated while on the wire forms a protoicicle, which is a stack of partially frozen hemispherical droplets with an assumed diameter $dd = 0.5$ cm (Maeno et al. 1994). The protoicicle freezes from the outside in, and when the surface water freezes the unfrozen interior water is retained and, as more heat is removed, eventually freezes. Assuming the surface layer of ice on the hemispherical droplets is 0.1 cm thick (Fig. 2, Maeno et al. 1994), the ratio of the volume of ice to the volume of the hemisphere is 0.64. In the heat-balance model, all the water in the protoicicle is incorporated in the icicle if the freezing fraction f_b, determined from the heat balance for the protoicicle, is greater than 0.64.

The convective and evaporative heat fluxes for this protoicicle are determined using Nu_{dd} for spheres. For forced convection (Incropera and DeWitt 1985, eq 7.55),

$$Nu_{dd} = 2 + Pr^{0.4}(0.4\, Re_{dd}^{1/4} + 0.06\, Re_{dd}^{2/3}), \quad (23)$$

and for free convection (Incropera and DeWitt 1985, eq 9.35),

$$Nu_{dd} = 2 + \frac{0.589 Ra_{dd}^{1/4}}{\left[1 + (0.469/Pr)^{9/16}\right]^{4/9}}. \quad (24)$$

The Sherwood number for vapor transfer is obtained from eq 23 and 24 using the heat and mass transfer analogy and replacing Pr with Sc both explicitly and in Ra_{dd} (Incropera and DeWitt 1985).

Of the other heat-flux terms, $Q_w = 0$ for icicles because the runoff water is already at 0°C. I assume that there is no solar radiation absorbed in the icicles, $Q_s = 0$, because a) the icicle orientation is close to vertical and thus roughly parallel to the incoming diffuse solar radiation flux, b) much of the longer-wavelength visible radiation is absorbed in the cloud cover, and c) very little of whatever incident shorter-wave radiation that gets through the clouds will be absorbed in the small-diameter clear icicle.

The fraction f_b of the available water that freezes is determined as in eq 21. If f_b is greater than 0.64 then all the available protoicicle water is retained, and if f_b is less than 0.64 the fraction of the protoicicle mass that is incorporated in the icicle is $f_b/0.64$.

After an icicle forms, runoff water may freeze to its sides. If there is wind, the Nusselt and Sherwood numbers for forced convection are determined using eq 7 and 13, based on the diameter of the icicle D_i. If there is no wind, heat transfer is by free convection. Heat transfer by free convection from the icicle (vertical cylinder) is different from that for the wire (horizontal cylinder). The relatively warm air at the surface of the icicle flows upward, drawing cooler air after it. The boundary layer thickness increases from the bottom to the top of the icicle, decreasing the heat transfer. The Nusselt number for free convection for this geometry is based on the length of the icicles rather than on their diameter. The appropriate icicle length to use is that for a single icicle, rather than this stack of icicles. Following Makkonen and Fujii (1993), I assume 45 identical icicles per meter of wire to give an average icicle length $L_{bar} = L_i/45$. Because the icicles are closely spaced on the wire, thus inhibiting cooling, I use an empirical formula for heat transfer from a vertical plate, rather than from a cylinder to determine the Nusselt number (Incropera and DeWitt 1985, eq 9.27):

$$Nu_{Lbar} = 0.68 + \frac{0.670 Ra_{Lbar}^{1/4}}{\left[1 + \left(\frac{0.492}{Pr}\right)^{9/16}\right]^{4/9}} \quad \text{for } Ra_{Lbar} < 10^9. \quad (25)$$

The Sherwood number for evaporative cooling is obtained from eq 25 by replacing Pr with Sc, both explicitly and in Ra_{Lbar}. The convective and evaporative heat fluxes are quite insensitive to the as-

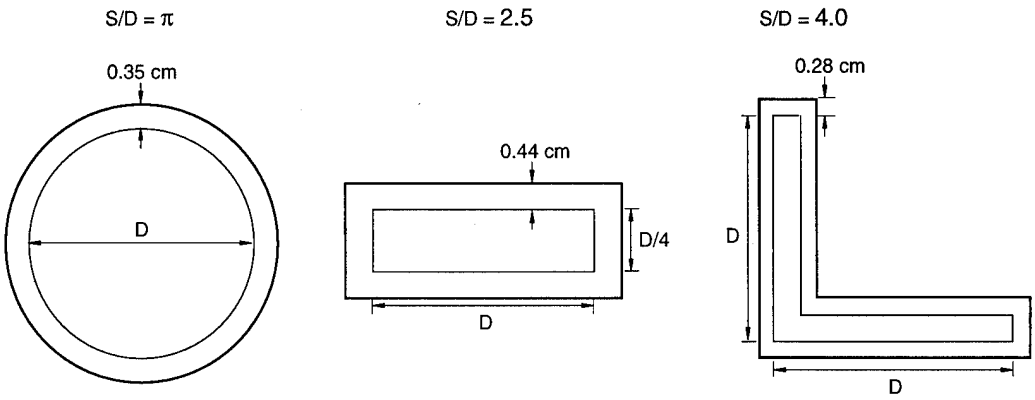

Figure 5. Equivalent uniform radial ice accretions on cylinders with circular, rectangular, and angle cross sections for a rainfall of 1 cm. The width of the rectangle is 1/4 of its length. The angle has equal-length legs with arbitrary thickness. The perimeter-to-"diameter" ratio S/D ranges from 3.14 for the circle to 2.5 for the rectangle and 4 for the angle.

sumed average icicle length as both h and h_m are proportional to $L_{bar}^{-1/4}$. As for the protoicicle, $Q_w = 0$ and $Q_s = 0$ and the freezing fraction f_s is determined using eq 21. The water that does not evaporate or freeze to the sides of the icicle forms a protoicicle at its tip, and the heat balance for the protoicicle is determined as before. Finally, the water that does not freeze at the tip is assumed to drip off. The new total icicle mass M_i is distributed evenly over a cylinder with length L_i equal to the original icicle length plus the length of the protoicicle.

6. SIMPLE FLUX MODEL

The simplest case of ice accreting in freezing rain occurs if all the precipitation impinging on the structure freezes in a uniform radial accretion. When that happens, the amount of ice on the structure is directly related to the amount of rain that falls. For example, if 1 cm of freezing rain falls on a 2-cm-wide flat plate and freezes in place, then a layer of ice $1(\rho_o/\rho_i) = 1.1$ cm thick results. On a 4-cm-wide plate nearby, the same thickness of ice would form with twice the mass. A 2-cm-diameter horizontal circular cylinder intercepts the same depth of rain as the 2-cm-wide flat plate. If that water depth is then spread uniformly around the cylinder's circumference and frozen, forming a uniform radial accretion, then the layer of ice is $1(\rho_o/\rho_i)/\pi = 0.35$ cm thick. The factor of π is the ratio between the circular cylinder's circumference, over which the ice freezes, and the diameter, which intercepts the precipitation. This calculation can be generalized to a cylinder with any cross section to determine the uniform ice thickness on its perimeter:

$$R_{eq} = \frac{D\rho_o}{S\rho_i} \sum_{j=1}^{N} \left(\frac{P_j}{10}\right) \Delta t \qquad (26)$$

where the summation gives the total precipitation amount in N hours and S and D are the perimeter and horizontal dimension, respectively, of the cross section. Equivalent uniform ice thicknesses are shown in Figure 5 for three different cross sections in a 1-cm rainfall.

For many shapes, but not circles, the D/S ratio decreases as ice accretes uniformly on the perimeter. For those, R_{eq} could be determined incrementally. When this is done for the rectangle in Figure 5, using 0.2-cm increments of rain, the final uniform radial ice thickness is 0.42 cm rather than 0.44 cm. This difference is well within the uncertainties in either this simple model or the detailed heat-balance model.

This simple precipitation model shows that, at least to first order, the thicknesses of ice on components with the same shape cross-section but different diameters are the same. On components with the same diameter but different cross sections, the ice thickness ratio is equal to the inverse of the perimeter ratio. Thus, uniform radial ice thicknesses determined by this model, or any other model, for a circular cylinder of any diameter can be extrapolated both to cylinders with other cross

sections and cylinders with other diameters.

A slightly more complex model takes the increased flux of water due to the horizontal velocity of the rain drops in the wind into account. Using the flux of precipitation from eq 3, the uniform radial ice thickness is

$$R_{eq} = \frac{D}{S\rho_i} \sum_{j=1}^{N} \left[\left(0.1 P_j \rho_o\right)^2 + \left(0.36 W_j V_j\right)^2 \right]^{1/2} \Delta t \ . \quad (27)$$

This simple flux model with $S/D = \pi$ is incorporated in ZRAIN for comparison with the heat-balance model.

7. COLLISION EFFICIENCY

In in-cloud icing, the collision efficiency of the cloud droplets with a structure is an important factor in determining the rate of ice accretion. Cloud droplets are very small, typically 5 to 50 μm in diameter, and have correspondingly small terminal velocities (0.007 m/s for 15 μm droplets, Best 1950). Thus, in windless conditions there is essentially no droplet flux. When there is wind, the wind drag on the droplets carries them along and the droplets follow the wind streamlines around any obstacle in their path. Only the inertia of the droplets, which tends to keep them moving in a straight-line path, makes them diverge from the wind streamlines. The collision efficiency of the cloud droplets with a structure represents a balance between their drag, the tendency to follow the streamlines, and their inertia, the tendency to continue in a straight line. Qualitatively, the results of this balance are that a) smaller droplets, which have less inertia, have lower collision efficiencies, b) the collision efficiency of droplets is smaller for large obstacles than for small ones, because streamlines diverge relatively farther in front of large obstacles than small ones, and c) in high winds droplets have more momentum so their collision efficiency is higher. These observations are quantified in Langmuir and Blodgett (1946). They numerically solved the trajectory equation, ignoring gravitational effects, to determine droplet collision efficiency as a function of two nondimensional numbers that depend on wind speed, wire diameter, droplet diameter, and the density and viscosity of air.

The Langmuir and Blodgett results cannot be applied to precipitation droplets. The terminal velocity of drizzle and rain drops, typically 100s of microns to 1 or 2 mm in diameter, is between about 2 and 7 m/s (Wang and Pruppacher 1977). Thus, even in no wind, there is a downward flux of water that is a balance between gravity and the drag of the still air on the drops. The drops fall through the air and collide either with the ground or with structures in their path. When there is wind, the drops gain horizontal velocity in addition to their vertical velocity. The effect of wind on drizzle- and rain-sized drops could be determined by numerically integrating the trajectory equation (Lozowski and Oleskiw 1983), including the gravitational term:

$$\frac{d\vec{v}}{dt} = -3\left[\frac{C_D \rho_a}{4 d \rho_o}\right] \left|\vec{v} - \vec{V}\right| \left(\vec{v} - \vec{V}\right) + \vec{g} \ , \quad (28)$$

where $\vec{v}$ is the drop velocity, $\vec{V}$ is the wind velocity, C_D is the drag coefficient of the drops, d is the drop diameter, and $\vec{g}$ is the acceleration of gravity. In the absence of a solution to this equation for rain- and drizzle-sized drops, it is reasonable to assume that the drops fall at their terminal velocity, move horizontally at the wind speed, and collide with all obstacles in their path.

In some freezing-rain ice accretion models, the collision efficiency of the rain and drizzle drops is calculated incorrectly. The resultant velocity of the wind speed and the drops' terminal velocity is used in the Langmuir and Blodgett (1946) formulation to determine the collision efficiency. This ignores the different physics of falling and wind-carried droplets and leads to obviously ridiculous results: 0.5-mm-diameter drizzle drops falling at 2 m/s in no wind are calculated to have a collision efficiency of 0.56 with a 1-m-diameter cylinder and 0.05 with a 10-m cylinder. In that world, if you carried a big enough umbrella, not only would you stay dry, so would the umbrella.

8. WIND LOAD

It is often important to know the wind load on a structure both during a freezing-rain storm, and for as long after the storm as ice remains on the structure. The projected area of the structure is larger because of the ice accretion, so at a given wind speed the wind load is greater than it would be on the bare structure. In ZRAIN, the wind load per meter of wire is determined every hour using the wire–ice diameter and the icicle diameter and length, assuming a drag coefficient $C_D = 1$ for both:

$$V_{load} = 0.5\rho_a V^2\left(D_c + D_i \frac{L_i}{100}\right). \quad (29)$$

The factor $L_i/100$ converts the wind load per length of icicle to wind load per meter of wire. The wind load results are useful for identifying the combination of wind and ice in each event that causes the highest horizontal load. This combination is independent of drag coefficient as long as it can be assumed to be the same for both the wire–ice accretion and the icicle.

9. SAMPLE RESULTS

ZRAIN was run for the freezing-rain events that occurred at the Des Moines, Iowa, airport between 1948 and 1993. The equivalent radial ice thicknesses on a 2.54-cm-diameter wire 10 m above the ground, hindcast using the heat-balance model, are shown in Figure 6 for the 316 freezing-rain events in those 45 years. For many events either no ice or very little ice accreted, even though freezing rain or drizzle was observed, typically because there was little or no measured precipitation. The largest accretion predicted by the model occurred in January 1982. That event consisted of two freezing-rain storms separated by 19 days of cold weather with temperatures as low as –30°C. In the first 12 hours of freezing rain, 0.75 cm of ice accreted, and in the second 19-hr period of freezing rain there was an additional 0.75-cm uniform radial accretion.

It is interesting to compare the modeled ice thicknesses with the *Storm Data* descriptions of the severe ice storms in 1990 and 1991. For the 7–8 March 1990 storm at the Des Moines airport, the heat-balance model hindcast a 0.5-cm-thick uniform radial accretion with 26-cm-long icicles (assuming 45 icicles/m), which is equivalent to a 1.3-cm uniform radial ice accretion. According to *Storm Data* this ice storm affected most of Iowa and resulted in 1.3 to 7.6 cm (0.5 to 3 in.) of ice on exposed surfaces and 7.6- to 12.7-cm (3- to 5-in.)-thick ice on some power lines. Central Iowa from near Des Moines and up to the north and west, particularly Carroll and Crawford counties (about 80 miles from Des Moines' Polk County), was hardest hit.

According to the model, the 31 October 1991 ice storm was less severe than the 1990 storm in the Des Moines area. The hindcast uniform radial ice accretion is only 0.2 cm thick with 3-cm-long icicles. *Storm Data* describes this ice storm as affecting about a third of Iowa, including the forecast zone where Des Moines is located. From 2.5 to 5.1 cm (1 to 2 in.) of ice accumulation was reported "in many areas," and much of the damage was attributed to the high winds that accompanied the storm. However, Des Moines' Polk County was not included in the Presidential Disaster Declaration for 43 Iowa counties following that storm (FEMA 1991), and the measured wind speeds at Des Moines airport were lower during this storm than in the 1990 storm.

The simple flux model results are compared with the heat-balance model results in Figure 7. The models agree well for the vast majority of the freezing-rain events at Des Moines. In the cases for which the results from the simple model are significantly higher than those from the heat-balance model, the air temperature was at or above 0°C with relative humidity near 100%, and moderate

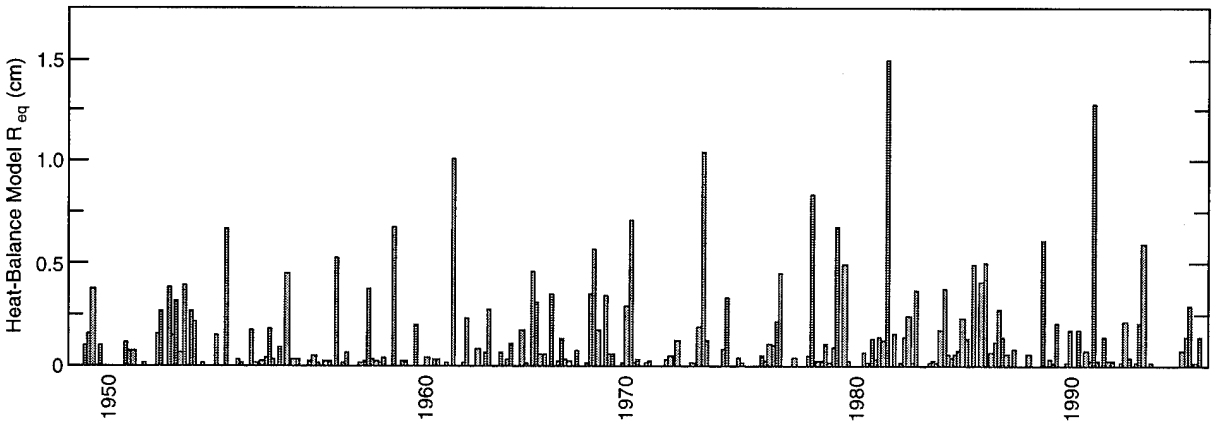

Figure 6. Uniform radial ice thicknesses hindcast by the heat-balance model for freezing-rain events at the Des Moines airport from 1948 to 1993.

or heavy precipitation. A time series of one of these events, the 7–8 March 1990 ice storm, is shown in Figure 8. This storm was characterized by high precipitation rates, up to 1 cm/hr, increasing temperature and relative humidity, and high diffuse solar radiation during the day. As the air temperature increased and freezing rain continued near the end of Julian day 66, little additional ice accreted directly on the wire, but much of the runoff water froze as icicles. It is during this time period that the heat-balance model results diverge from the simple flux model, which accretes all the impinging precipitation.

The heat-balance model was also run for a 10-cm-diameter wire to determine whether the lack of dependence of the ice thickness on wire diameter predicted by the simple model also holds when the heat fluxes, which are diameter-dependent (Fig. 3), are incorporated in the ice accretion calculation. The equivalent radial thicknesses for these two diameters are compared in Figure 9 and show almost no difference. This is undoubtedly due to the accretion of runoff water as icicles, which freeze independent of the wire diameter.

One small but well-documented freezing-rain event at CRREL on 28 February 1995 serves as a test for the two models against reality. This event was characterized by cold temperatures, very light winds, and light freezing drizzle that froze quickly rather than as icicles. The ice thickness determined from the measured mass of ice on a 2.65-cm-diameter horizontal rod (Itagaki, in prep.) at CRREL's freezing-rain weather station was 0.19 cm. Both models predict equivalent radial ice accretions 0.18-cm thick. While this good agreement is encouraging, further testing of the models in more extreme freezing-rain conditions is desirable.

10. DISCUSSION

This report describes two models to calculate freezing-rain ice loads on horizontal cylinders from weather data. One model is very simple and requires only the information that freezing rain is occurring along with the concurrent precipitation rate and wind speed. The more detailed model requires as additional information the air temperature, dew-point temperature, and solar radiation flux, as well as the diameter of the wire on which ice is accreting. A comparison of the two models using the historical weather data at Des Moines indicates that the simple flux model is conservative, as expected, but generally agrees well with the detailed heat-balance model.

As freezing-rain events occur at CRREL, measurements of accreted ice on horizontal rods will be compared with the models' predictions. This

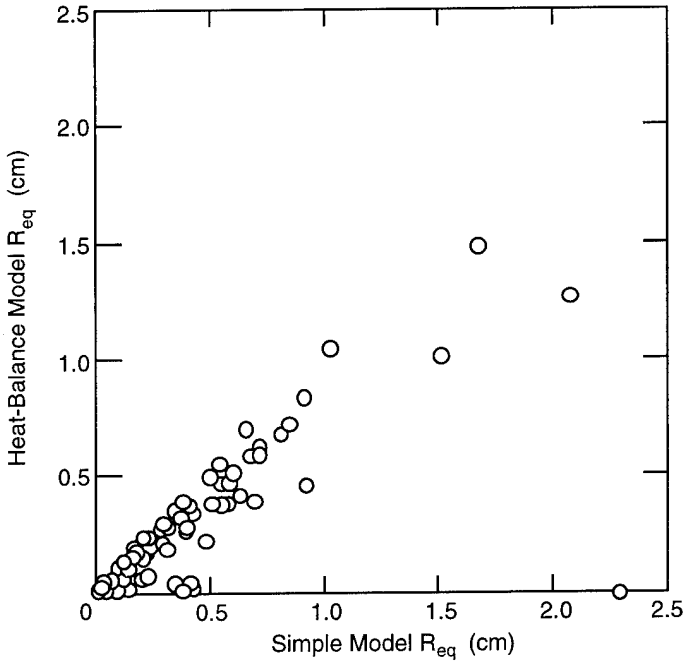

Figure 7. Comparison of uniform radial ice thicknesses at Des Moines from the simple flux model and the heat-balance model.

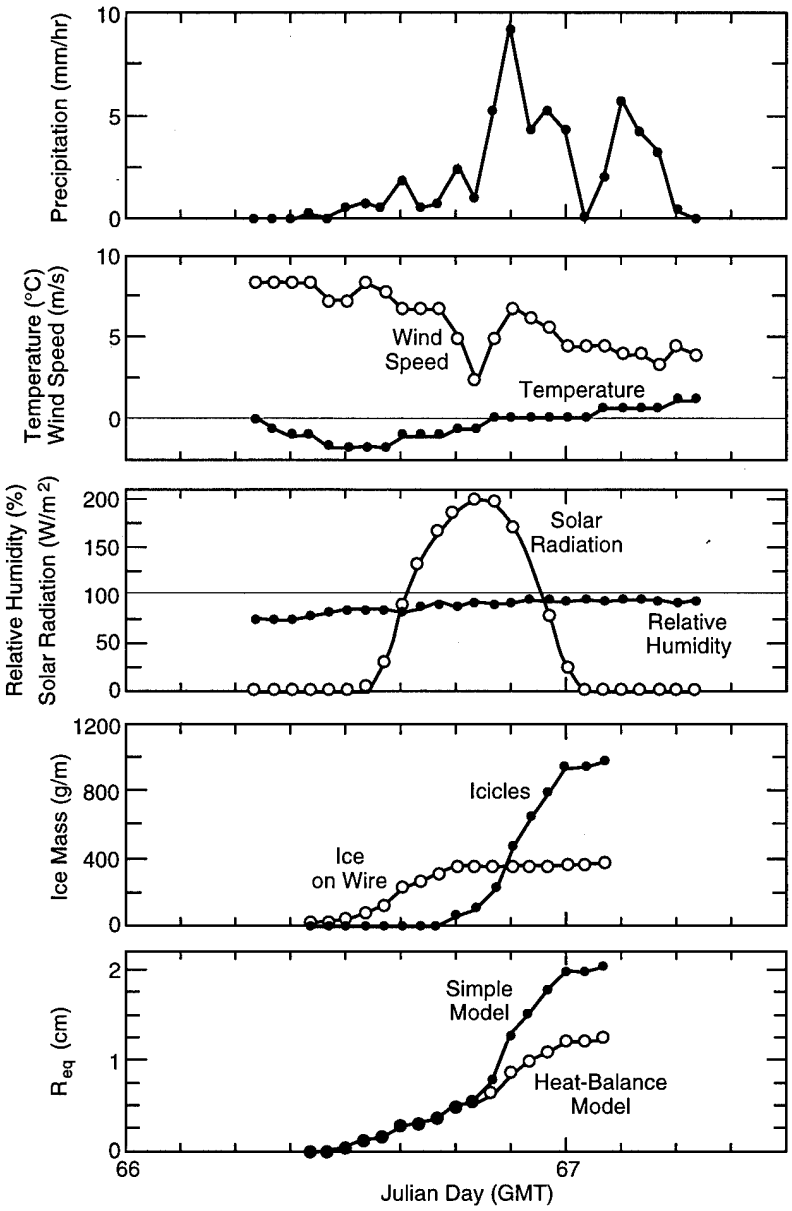

Figure 8. Time series of the weather conditions and hindcast ice accretions for the ice storm of 7–8 March 1990 at the Des Moines airport. The formation of icicles in the heat-balance model occurs in relatively warm, humid conditions. In those conditions the results from the heat-balance model and the simple flux model diverge.

field data can be used to fine-tune the heat-balance model. Parameters that may have a significant effect on the calculated ice load and may need to be adjusted, include a) the 0.64 threshold for incorporating all of the runoff water in the protoicicle, and b) the projected area of the ice accretion that is assumed to intercept the precipitation flux.

The good agreement between the heat-balance model and the simple flux model is interesting. It indicates that the modeled ice thicknesses can be easily extrapolated so that consistent ice thicknesses can be used in the design of structural elements with different cross sections. It also shows that weather data can be used to determine conservative, but apparently realistic, ice loads using back-of-the-envelope calculations. It will be interesting to see if this good agreement holds as the heat-balance model is fine-tuned.

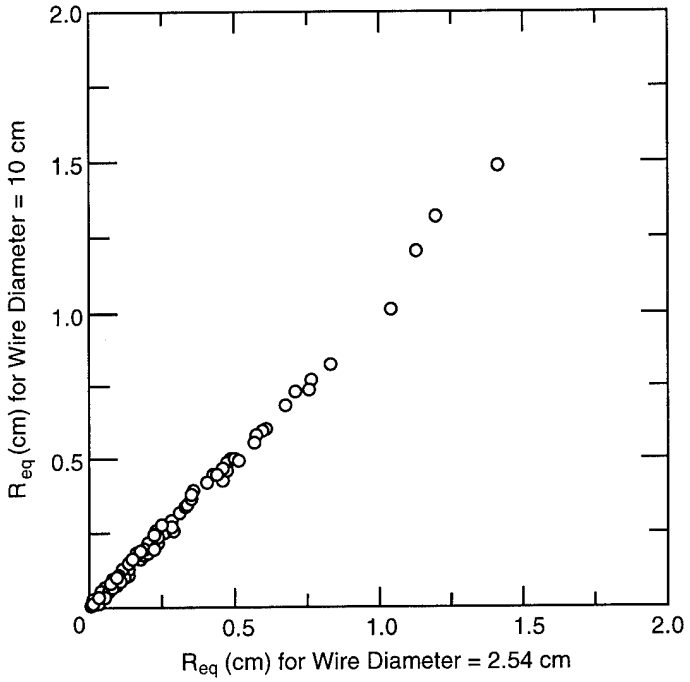

Figure 9. Comparison of uniform radial ice accretion thicknesses for 2.54- and 10-cm-diameter wires using the heat-balance model.

LITERATURE CITED

Ackley, S.F. and K. Itagaki (1970) Distribution of icing in the Northeast's ice storm of 26–27 December 1969. *Weatherwise*, **23**: 274–279.

Achenbach, E. (1977) The effect of surface roughness on the heat transfer from a circular cylinder to the crossflow of air. *International Journal of Heat and Mass Transfer*, **20**: 359–369.

ASCE (1991) *Guidelines for Electrical Transmission Line Structural Loading*. ASCE Manuals and Reports on Engineering Practice No. 74, American Society of Civil Engineers, New York.

ASCE (1994) *Minimum Design Loads for Buildings and Other Structures*. ASCE Standard 7-93, American Society of Civil Engineers, New York.

Batchelor, G.K. (1970) *An Introduction to Fluid Dynamics*. New York: Cambridge University Press.

Bennett, I. (1959) *Glaze: Its Meteorology and Climatology, Geographical Distribution and Economic Effects*. Quartermaster Research and Engineering Center, Environmental Protection Research Division, Technical Report EP-105.

Best, A.C. (1949) The size distribution of raindrops. *Quarterly Journal of the Royal Meteorological Society*, p. 16–36.

Best, A.C. (1950) The size of cloud droplets in layer-type clouds. *Quarterly Journal of the Royal Meteorological Society*, p. 241–248.

Buck, A. (1981) New equations for computing vapor pressure and enhancement factor. *Journal of Applied Meteorology*, **20**: 1527–1532.

EIA/TIA (1991) *Structural Standards for Steel Towers and Antenna Supporting Structures*. EIA/TIA-222-E, Electronics Industries Association, Washington, D.C.

FEMA (1991) *Hazard Mitigation Opportunities in Iowa*. FEMA-928-DR-Iowa, Kansas City, Missouri.

IEC (1990) *Loading and Strength of Overhead Transmission Lines*. International Standard 826, 2nd edition. International Electrotechnical Commission, Technical Committee 11, Geneva, Switzerland.

Incropera, F.P. and D.P. DeWitt (1985) *Fundamentals of Heat and Mass Transfer*. New York: John Wiley and Sons.

Iqbal, M. (1983) *An Introduction to Solar Radiation*. Don Mills, Ontario: Academic Press Canada.

Itagaki, K. (in prep.) Mass measurement of wet snow and freezing rain accumulation.

Langmuir, I. and K. Blodgett (1946) Mathematical investigation of water droplet trajectories. In *The Collected Works of Irving Langmuir* (C.G. Suits, Ed.) (1960), p. 335–393. Elmsford, New York: Pergamon Press.

Lozowski, E.P. and M.M. Oleskiw (1983) *Computer modeling of time dependent rime icing in the atmosphere.* CRREL Report 83-2, Cold Regions Research and Engineering Laboratory, Hanover, New Hampshire.

Lozowski, E.P., E.M. Gates and L. Makkonen (1987) Recent progress in the incorporation of convective heat transfer into cylindrical ice accretion models. In *1987 International Symposium on Cold Regions Heat Transfer,* American Society of Mechanical Engineers.

Maeno, N., L. Makkonen, K. Nishimura, K. Kosugi and T. Takahashi (1994) Growth rates of icicles. *Journal of Glaciology,* **40**(135): 319–326.

Makkonen, L. (1984) Modeling of ice accretion on wires. *Journal of Climate and Applied Meteorology,* **23**: 929–939.

Makkonen, L. and Y. Fujii (1993) Spacing of icicles. *Cold Regions Science and Technology,* **21**: 317–322.

Marshall, J.S. and W. Palmer (1948) Relation of drop size to intensity. *Journal of Meteorology,* **5**: 165–166.

Morgan, V.T. (1973) The heat transfer from bare stranded conductors by natural and forced convection in air. *International Journal of Heat and Mass Transfer,* **16**: 2023–2034.

Morgan, V.T. (1975) The overall convective heat transfer from smooth circular cylinders. In *Advances in Heat Transfer* (T.F. Irvine and J.P. Hartnett, Eds.), vol. 11, p. 199–264. New York: Academic Press.

MRI (1977) *Pacific Northwest Icing Study,* MRI 77 FR-1515, prepared for Bonneville Power Administration, Portland, Oregon.

NOAA (1959–1995) *Storm Data and Other Unusual Weather Phenomena.* National Climate Data Center, Asheville, North Carolina.

NOAA (1993) Solar and Meteorological Surface Observation Network 1961–1990 Version 1.0. September. National Climate Data Center, Asheville, North Carolina.

NOAA (yearly) *Local Climatological Data Annual Summary.* National Climate Data Center, Asheville, North Carolina.

Pruppacher, H.R. and J.D. Klett (1980) *Microphysics of Clouds and Precipitation.* Boston: D. Reidel Publishing Co.

Southeast Regional Climate Center (1993) *Freezing Rain and Sleet Climatology of the Southeastern United States.* NOAA, Columbia, South Carolina.

Tattelman, P. and I.I. Gringorten (1973) *Estimated Glaze Ice and Wind Loads at the Earth's Surface for the Contiguous United States.* Air Force Cambridge Research Laboratories Report AFCRL-TR-73-0646.

Vilcans, J. and D. Burnham (1989) *Climatological study to determine the impact of icing on the Low Level Windshear Alert System.* DOT-TSC-FAA-89-2, U.S. Department of Transportation.

Wang, P.K. and H.R. Pruppacher (1977) Acceleration to terminal velocity of cloud and rain drops. *Journal of Applied Meteorology,* **16**: 275–280.

APPENDIX A: COMPARISON OF EVAPORATIVE HEAT FLUX FORMULATIONS

The formulation of the evaporative heat flux term in the heat-balance model is different from that of Lozowski et al. (1987) and Makkonen (1984). The different Q_es are compared in this appendix. Assuming consistent units and considering the heat flux across an arbitrary surface, Q_e is (eq 4)

$$Q_e = h_m L_e \left(\frac{e_0}{273.15} - \frac{Rhe_T}{T + 273.15} \right) \frac{m_w}{R} , \tag{A1}$$

Using the definition of the Sherwood number Sh_D and the relationship between Sh_D and the Nusselt number Nu_D specified by the heat and mass transfer analogy gives

$$\begin{aligned} Nu_D &= hD/k_a = CPr^{0.37} Re_D{}^b \\ Sh_D &= h_m D/\kappa_m = CSc^{0.37} Re_D{}^b \end{aligned} \tag{A2}$$

where C and b depend on Re_D. Equation A2 can be used to write h_m in terms of Nu_D:

$$h_m = \frac{\kappa_m Nu_D \left(\frac{Sc}{Pr} \right)^{0.37}}{D} . \tag{A3}$$

Using this relationship and $Sc/Pr = k_a/(\rho_a c_p \kappa_m)$, eq A1 can be written finally as

$$Q_e = \frac{Nu_D}{D} \left(\frac{k_a}{\rho_a c_p} \right)^{0.37} \kappa_m{}^{0.63} \frac{m_w L_e}{R} \left(\frac{e_0}{273.15} - \frac{Rhe_T}{T + 273.15} \right) . \tag{A4}$$

The evaporative heat transfer term in Lozowski et al. (1987) is given as

$$Q_e = h \left(\frac{Pr}{Sc} \right)^{0.63} \varepsilon L_e \left(\frac{e_0 - Rhe_T}{c_p Pa} \right) , \tag{A5}$$

where $\varepsilon = m_w/m_a$ is the ratio of the molecular weights of water vapor and air. Using the ideal gas law,

$$Pa = \frac{\rho_a R(T + 273.15)}{m_a} , \tag{A6}$$

and the definition of Nu_D in eq A2, eq A5 becomes

$$Q_e = \frac{Nu_D}{D} \left(\frac{k_a}{\rho_a c_p} \right)^{0.37} \kappa_m{}^{0.63} \frac{m_w L_e (e_0 - Rhe_T)}{R(T + 273.15)} . \tag{A7}$$

Thus, Lozowski and Gates's formulation (eq A7) is different from this model's formulation (eq A4) only in the temperature used to calculate the saturation vapor density at the accretion surface.

In Makkonen (1984) the evaporative cooling flux is given as

$$Q_e = \frac{h \varepsilon L_e (e_0 - e_T)}{c_p Pa} . \tag{A8}$$

Again using the ideal gas law and eq A2, this can be rewritten as

$$Q_e = \frac{Nu_D}{D}\left(\frac{k_a}{\rho_a c_p}\right)\frac{m_w L_e (e_0 - e_T)}{R(T + 273.15)}. \qquad \text{(A9)}$$

Makkonen's formulation differs from this model's by the temperature used to calculate the saturation vapor density at the freezing surface, by the dependence on $k_a/(\rho_a c_p)$ rather than on $[k_a/(\rho_a c_p)]^{0.37}\kappa_m^{0.63}$, and by using the saturation vapor density of the air rather than the vapor density at the ambient humidity.

The effect of these differences is to make Lozowski and Gates's Q_e 4% larger and Makkonen's Q_e 32% smaller than this model's at typical freezing-rain conditions $T = -3°C$, $Rh = 90\%$ and $Pa = 1000$ mbar. The differences between the models increase somewhat as air temperature decreases and increase substantially as humidity decreases.

This comparison addresses the differences in the physical models of evaporative cooling and in the assumed dependence of the Nusselt number on the Prandtl and Schmidt numbers. There are further differences between the models in the empirical formulas used to relate the Nusselt number to the Reynolds number and Rayleigh number.

APPENDIX B: SKY DIFFUSE SOLAR RADIATION FLUX TO A HORIZONTAL CYLINDER

Sky diffuse radiation under an overcast that would be typical during freezing rain is approximately isotropic over the sky dome. The flux of diffuse solar radiation to a surface inclined at an angle α to the horizontal (Fig. B1) is

$$Q_{st} = Sr(1 + \cos\alpha)/2 \tag{B1}$$

for the top of the surface, and

$$Q_{sb} = Sr(1 - \cos\alpha)/2 \tag{B2}$$

for the bottom of the inclined surface (Iqbal 1983). The circumference of a cylinder is made up of elements with area $dC = Dd\alpha/2$ per unit length, inclined at angles to the horizontal varying from $-\pi/2$ to $\pi/2$ (Fig. B2). The contributions of the sky diffuse solar radiation to each of these surface elements are summed, taking advantage of the symmetry of the cylinder about the vertical, to determine the solar power per unit length of the cylinder:

$$P_s = Sr\left[2\left(\frac{D}{2}\right)\int_0^{\pi/2}\left(\frac{1+\cos\alpha}{2}\right)d\alpha + 2\left(\frac{D}{2}\right)\int_{-\pi/2}^{0}\left(\frac{1-\cos\alpha}{2}\right)d\alpha\right]. \tag{B3}$$

Evaluating the integrals results in $P_s = \pi DSr/2$, so the flux of sky diffuse solar radiation to the cylinder per diameter is

$$Q_s = \frac{\pi Sr}{2}, \tag{B4}$$

which was given in eq 4.

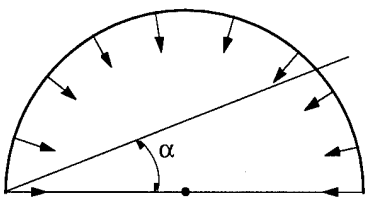

Figure B1. Sky diffuse solar radiation incident on surface inclined at an angle α to the horizontal.

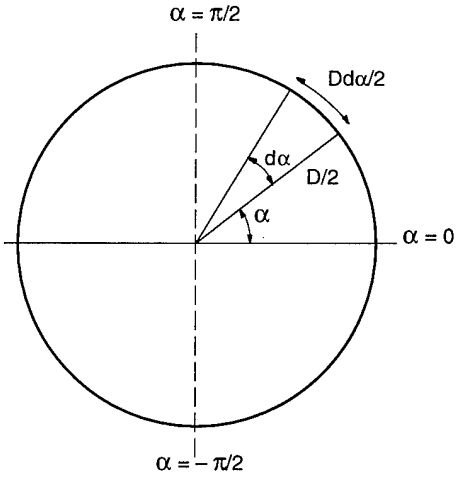

Figure B2. Cylinder surface elements.

REPORT DOCUMENTATION PAGE

Form Approved
OMB No. 0704-0188

1. AGENCY USE ONLY (Leave blank)	2. REPORT DATE	3. REPORT TYPE AND DATES COVERED
	April 1996	

4. TITLE AND SUBTITLE
Ice Accretion in Freezing Rain

5. FUNDING NUMBERS
PR: 4A762784AT42
WU: CS-W03

6. AUTHORS
Kathleen F. Jones

7. PERFORMING ORGANIZATION NAME(S) AND ADDRESS(ES)
U.S. Army Cold Regions Research and Engineering Laboratory
72 Lyme Road
Hanover, N.H. 03755-1290

8. PERFORMING ORGANIZATION REPORT NUMBER
CRREL Report 96-2

9. SPONSORING/MONITORING AGENCY NAME(S) AND ADDRESS(ES)

10. SPONSORING/MONITORING AGENCY REPORT NUMBER

11. SUPPLEMENTARY NOTES

12a. DISTRIBUTION/AVAILABILITY STATEMENT
Approved for public release; distribution is unlimited.
Available from NTIS, Springfield, Virginia 22161

12b. DISTRIBUTION CODE

13. ABSTRACT (*Maximum 200 words*)

Ice accreted on structures from freezing rain causes both increased vertical loads and increased wind loads, due to the larger projected area of the structure. Structural failures initiated by ice loads frequently cause millions of dollars of damage to overhead power and communication lines, towers, and other ice-sensitive structures. There is little information on ice loads to use in the design of these structures, so freezing-rain models have been developed for use with weather measurements to determine the severity of accreted ice loads from historical data. This report describes a detailed heat-balance ice accretion model, including the important heat fluxes in freezing rain and allowing the accretion of runoff water in the form of icicles. It also presents a simple algorithm for calculating the ice load on components with different diameters and cross sections. Collision efficiency in freezing rain and the calculation of the wind-on-ice load are also discussed. Model results are compared with the ice load measured during a recent freezing rain storm, and to each other, using 45 years of weather data from Des Moines, Iowa.

14. SUBJECT TERMS				15. NUMBER OF PAGES
	Collision efficiency	Ice load	Wind-on-ice load	31
	Freezing rain	Icicles		16. PRICE CODE
	Ice	Rain		

17. SECURITY CLASSIFICATION OF REPORT	18. SECURITY CLASSIFICATION OF THIS PAGE	19. SECURITY CLASSIFICATION OF ABSTRACT	20. LIMITATION OF ABSTRACT
UNCLASSIFIED	UNCLASSIFIED	UNCLASSIFIED	UL